ELSEVIER

Chemical Engineering Journal 85 (2002) 189–195

Chemical Engineering Journal

www.elsevier.com/locate/cej

An inverse approach for estimation of the surface heat flux distribution on a horizontal elliptical tube with laminar film condensation

Pao-Tung Hsu [a,*], Yih-Hsiung Liu [b], Sheng-Gwo Wang [b], Cha'o-Kuang Chen [c]

[a] *Department of Industrial Management, Shu-Te University, No. 59, Hun-Shan Road, Hun-Shan Village, Yen Chau, Kaohsiung County, Taiwan*
[b] *Mechanical Engineering Department, Kaohsiung University of Applied Sciences, Kaohsiung, Taiwan*
[c] *Mechanical Engineering Department, National Cheng Kung University, Tainan, Taiwan*

Received 22 February 2000; received in revised form 17 February 2001; accepted 19 February 2001

Abstract

A direct method is developed for determining the wall heat flux in film condensation on a horizontal elliptical tube. A finite-difference method is employed to discretize the condensation domain, and then a linear inverse model is constructed to identify the unknown conditions. The inverse analysis is based on the assumption that the film thickness measurements are available over the domain. Our approach is to rearrange the matrix forms of the differential governing equation and estimate the unknown surface conditions. Then, the linear least-squares method is adopted to find the solution. For condensation problem, the governing equation is non-linear. The present woke proposes a transformed treatment for solving both inverse and direct problems.

In contrast to the traditional approach, the advantage of this method in inverse analysis is that no prior information is needed on the functional form of the unknown quantities, no initial guess is required and the iterations of calculation process need be done only once. Finally, the effects of measurement errors, sensor positions and the measurement points on the inverse solutions are discussed.

Keywords: Inverse approach; Least-squares method; Heat flux; Condensation

1. Introduction

The original Nusselt's [1] model for film condensation of a quiescent vapor along an isothermal vertical plate equated gravity and viscous forces. A number of systems, such as plates, and bank of tubes, have been extensively studied under various conditions by many investigators. As for horizontal elliptical tube surfaces, Wang et al. [2] showed theoretically and experimentally that an elliptical tube did possess some advantages over a cylindrical one. Later, Yang and Chen [3–5] investigated laminar film condensation on horizontal elliptical tubes.

Beck et al. [6] showed that if the heat flux or temperature at the surface of a solid are known, then the temperatures distribution can be found. This is termed a direct problem. If the surface heat flux or temperature of a solid must be determined from the temperature measurements at one or more locations at the surface, this is an inverse problem. However, the condensation problems analyzed thus have been limited to the direct problem. No work is available in the area of inverse analysis of film condensation. In such cases, the inverse analysis of a heat transfer problem can provide a powerful technique to estimate the unknown conditions.

Various methods have been employed to handle the inverse heat conduction problem (IHCP); these include analytical or numerical approaches, such as graphical [7], polynomial [8], Laplace transform [9], finite difference and finite element [10,11], regularization methods [12], and conjugate gradient iterative method [13], direct sensitivity coefficient method [14].

In order to remedy, at least in part, the lack of literature in this field, this paper continues the study of a recently presented methodology for solving IHCP. This method [15,16] rearranges the matrix forms of the direct problem in order to represent the unknown conditions explicitly. Then, the inverse model can be used to solve through the least-squares error method. In general, the governing equation of the IHCP is linear, but in the condensation problem, the governing equation is non-linear. The present work proposes a transformed treatment for solving both inverse and direct problems. The advantage of applying this method in inverse

* Corresponding author. Present address: Industrial Management Department, Shu-Te University, No. 59, Hun-Shan Road, Hun-Village, Yen Chau, Kaohsiung Country Taiwan Tel.: +886-7-615-1000x4515; fax: +886-7-615-1000x4599.

1385-8947/02/$ – see front matter
PII: S1385-8947(01)00151-6

Nomenclature

A	matrix is the function of thermal properties
B	the coefficient matrix of θ
a, b	semimajor, semiminor axis of ellipse
c_p	heat capacity
e	an ellipticity of the ellipse
g	the acceleration of gravity
h_{fg}	the latent heat of condensation
k	thermal conductivity
N	measuring points
$q(\phi)$	wall heat flux
R	the reverse matrix of the inverse problem
$\bar{T}$	the liquid filmwise thickness distribution of the wall

Greeks

α	thermal diffusivity
δ	the thickness of the liquid film
ϕ	the angle between the tangent to tube surface and the normal to direction of gravity
θ	the angle measured from the tube upper generatrix
θ	matrix is the function of the boundary
$\bar{\boldsymbol{\theta}}$	the coefficient vector of $q(\phi)$
μ	the dynamic viscosity of liquid
ρ	density
σ	the random error of the β
ω	measurement error

Subscript

i	index of ϕ-axial coordinate

analysis is that no prior information is needed on the functional form of the unknown quantities, no initial guess has to be used and the number of iterations of the calculation process is limited to 1. Furthermore, the effects of sensor position, magnitude of measurement error and the number of measurements on the accuracy of estimates are examined.

2. Analysis

2.1. Description of the mathematical model

Consider the pure quiescent vapor at saturated state with saturated temperature T_s condensing on a horizontal elliptical tube, with major axis $2a$ in the direction of gravity and minor axis $2b$. The variable heat flux is through the wall over the entire length of the tube. Thus, condensation occurs on the wall and a continuous film of the liquid runs downward over the tube under the influence of gravity. The physical model under consideration is shown in Fig. 1, where the curvilinear coordinates (x, y) are aligned along the elliptical wall surface and its normal. The steady-state laminar film

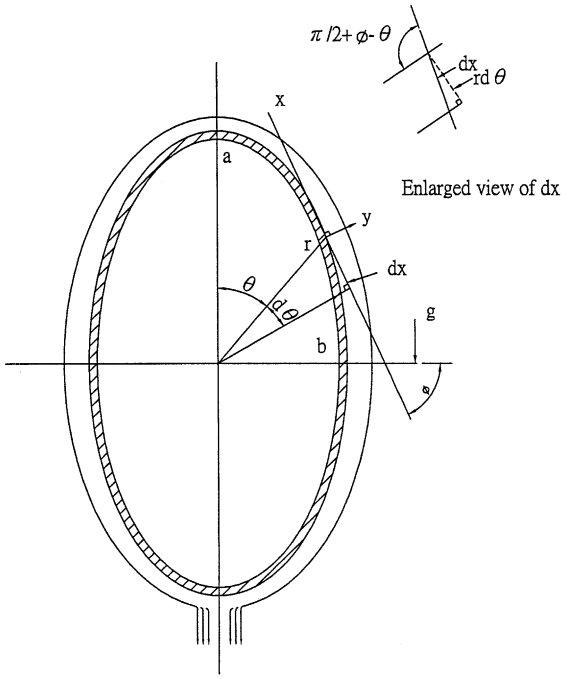

Fig. 1. Schematic and coordinate system for the condensate film flow on the elliptical surface.

condensation layer have constant fluid properties. Additional assumptions are essentially those of Nusselt's classical analysis: (1) the inertia and convection terms are neglected; (2) subcooling of the condensate may be neglected: (3) the interfacial shear forces on the vapor–liquid interface and surface tension force are neglected. Thus it have the following governing equations for the condensate film:

Momentum equation

$$0 = \mu \frac{\partial^2 u}{\partial y^2} + \rho g \sin\phi \tag{1}$$

where μ is the dynamic viscosity of the liquid, ρ the density of liquid and g the acceleration of gravity.

Energy equation

$$\frac{\mathrm{d}}{\mathrm{d}x}\int_0^{\delta} \rho u h_{fg}\,\mathrm{d}y = q(x)|_{y=0} \tag{2}$$

where h_{fg} is the latent heat of condensation; $q(x)$ the surface heat flux and δ the thickness of the liquid film.

The velocity distribution in the film flowing across the surface can be obtained by integrating Eq. (1) and with the boundary conditions $u = 0$ at $y = 0$ and $\partial u/\partial y = 0$ at $y = \delta$ (no interfacial shear):

$$u = \frac{\rho g}{\mu}\delta^2 \sin\phi \left[\frac{y}{\delta} - \frac{1}{2}\left(\frac{y}{\delta}\right)^2\right] \tag{3}$$

Substituting Eq. (3) into Eq. (2) yields

$$\frac{1}{3}\frac{\rho^2 g h_{fg}}{\mu}\frac{\mathrm{d}}{\mathrm{d}x}(\delta^3 \sin\phi) = q(x)|_{y=0} \tag{4}$$

where $\phi = \phi(x)$ is the angle between the normal to gravity and the tangent to the tube wall at the position (r, θ). Here, θ is the angle measured from the tube upper generatrix; r the radial distance from the centroid of the ellipse and can be expressed as

$$r = a\left[\frac{1-e^2}{1-e^2\cos^2\theta}\right]^{0.5} \tag{5}$$

where $e = \sqrt{a^2-b^2}/a$ is an ellipticity of the ellipse. With reference to Fig. 1, the differential elliptical arc length

$$\mathrm{d}x = \frac{r\,\mathrm{d}\theta}{\cos(\phi-\theta)} \tag{6}$$

By using the geometric relationship for tangent to the elliptical surface, one has

$$\tan\phi = \frac{\tan\theta}{1-e^2} \tag{7}$$

Substituting Eqs. (5)–(7) into Eq. (4), and introducing a transformation of variable from x to ϕ, one obtains the energy equation as follows:

$$\frac{\rho^2 g}{3\mu}\frac{h_{\mathrm{fg}}}{a(1-e^2)}(1-e^2\sin^2\phi)^{3/2}\frac{\mathrm{d}}{\mathrm{d}\phi}(\delta^3\sin\phi) = q(\phi)|_{y=0} \tag{8}$$

Eq. (8) is subject to the boundary conditions

$$\frac{\mathrm{d}\delta}{\mathrm{d}r} = 0 \quad \text{at } \phi = 0 \tag{9}$$

Eq. (8) is non-linear, if let $\beta = \delta^3\sin\phi$, then Eq. (8) becomes linear, and can be written as

$$\frac{\mathrm{d}\beta}{\mathrm{d}\phi} = \frac{1}{(\rho^2 g/3\mu)(h_{\mathrm{fg}}/a(1-e^2))(1-e^2\sin^2\phi)^{3/2}}q(\phi)|_{y=0} \tag{10}$$

And the boundary condition equation (9) may be transferred as follows:

$$\frac{\mathrm{d}\beta}{\mathrm{d}\phi} = 0 \quad \text{at } \phi = 0 \tag{11}$$

The above boundary conditions are given except for $q(\phi)$, which is unknown to be estimated.

2.2. The direct problem

The finite-difference method is employed to discretized the above governing equation (Eq. (10)) combined with the boundary conditions. It can be expressed as the following recursive forms:

$$\frac{1}{\Delta\phi}(\beta_{i+1}-\beta_i) = \frac{1}{(\rho^2 g/3\mu)(h_{\mathrm{fg}}/a(1-e^2))(1-e^2\sin^2\phi)^{3/2}}q(\phi)|_{y=0} \tag{12}$$

where $\Delta\phi$ is the increments in the spatial coordinate, i the ith grid along the ϕ coordinate, and $\beta_i = \delta_i^3\sin\phi_i$, δ_i the liquid film thickness at the grid point (i).

Using the recursive forms, an equivalent matrix equation can be expressed as

$$\mathbf{A}\bar{T} = \boldsymbol{\theta} \tag{13}$$

where the matrix $\mathbf{A}$ is the function of thermal properties and the scale of the position. The components of $\bar{T}$ are the β_i in discretized points, and the components of $\boldsymbol{\theta}$ are the function of the boundary conditions. Thus Eq. (13) can be written as follows:

$$\begin{bmatrix} E & & & & \\ -E & E & & & \\ & -E & E & & \\ & & \ddots & \ddots & \\ & & & -E & E \end{bmatrix}\begin{bmatrix}\beta_1\\ \beta_2\\ \beta_3\\ \vdots\\ \beta_n\end{bmatrix} = \begin{bmatrix} Fq_1\\ Fq_2\\ Fq_3\\ \vdots\\ Fq_n\end{bmatrix} \tag{14}$$

where $E = 1/\Delta\phi$, $\beta_i = \delta_i^3\sin\phi_i$, and

$$F = \frac{1}{(\rho^2 g/3\mu)(h_{\mathrm{fg}}/a(1-e^2))(1-e^2\sin^2\phi)^{3/2}}$$

The direct problem considered here is concerned with the determination of the β_i at the nodes when all boundary conditions, and other thermal properties are known. The above direct problem of Eq. (13) can then be solved using Gauss elimination method.

2.3. The inverse problem

This inverse problem is to identify the applied heat flux $q(\phi)$ from the liquid film thickness ($\beta_i = \delta_i^3\sin\phi_i$) measurements taken at the different points of the surface. Suppose that the applied heat flux $q(\phi)$ is represented as the following series forms or non-form (i.e. the heat flux $q(\phi)$ is not necessary to be a regular form) in the problem domain:

$$q(\phi) = \sum_{i=0}^{N} a_i\zeta_i(\phi) \quad \text{(or non-form)} \tag{15}$$

where $\zeta_i(\phi)$ is a non-singular function in the problem domain.

For an inverse problems, $\mathbf{A}$ can be constructed according to the known physical model and numerical methods, and $\bar{T}$ can be calculated by $\beta_i = \delta_i^3\sin\phi_i$. The liquid film thickness (δ_i) is taken at the different points of the surface by the sensor. The coefficients of $q(\phi)$ are the main tasks to resolve. The coefficients of $q(\phi)$ from $\boldsymbol{\theta}$ will transfer the direct formulation to the following inverse forms:

$$\mathbf{A}\bar{T} = \mathbf{B}\bar{\boldsymbol{\theta}} \tag{16}$$

$$\mathbf{B}\bar{\boldsymbol{\theta}} = \begin{bmatrix} F & & & \\ & F & & \\ & & \ddots & \\ & & & F \end{bmatrix} \begin{bmatrix} q_1 \\ q_2 \\ \vdots \\ q_n \end{bmatrix} \tag{17}$$

where $\boldsymbol{\theta} = \mathbf{B}\bar{\boldsymbol{\theta}}$, $\mathbf{B}$ is the coefficient matrix of $\bar{\boldsymbol{\theta}}$ and $\bar{\boldsymbol{\theta}}$ is the coefficient vector of $q(\phi)$, then $\bar{\boldsymbol{\theta}}$ can be solved by the least-squares error method as follows:

$$\bar{\boldsymbol{\theta}} = [(\mathbf{A}^{-1}\mathbf{B})^{\mathrm{T}}(\mathbf{A}^{-1}\mathbf{B})]^{-1}(\mathbf{A}^{-1}\mathbf{B})^{\mathrm{T}}\mathbf{T} = \mathbf{R}\mathbf{T} \tag{18}$$

where $\mathbf{R} = [(\mathbf{A}^{-1}\mathbf{B})^{\mathrm{T}}(\mathbf{A}^{-1}\mathbf{B})]^{-1}(\mathbf{A}^{-1}\mathbf{B})^{\mathrm{T}}$, it is the reverse matrix of the inverse problems.

Eq. (16) is assumed to measure all discretized points, and let $\beta = \delta^3 \sin\phi$ in the problems. In most cases, not all of the points need to be measured. Therefore, only part of matrix $\mathbf{R}$ and $\mathbf{T}$, and part of vector $\bar{\boldsymbol{\theta}}$ that correspond to the measuring positions need be constructed. In general, when a large portion of the matrices and vector are selected, i.e. the number of transducers or measuring points is large, the costs of computation and experiment increase. However, a large number of measuring points yields increased accuracy of the estimated results.

When the rank of the reverse matrix is equal to the number of the unknown variables, then: (1) if the matrix equation (16) is consistent, a solution exists and is unique;(2) if the matrix equation is inconsistent, a unique least-squares solution can be approximated.

3. Results and discussion

The inverse film condensation problem defined by Eqs. (1) and (2) and are used in the following examples to verify the accuracy, efficiency, and versatility of the proposed method for estimating the unknown conditions of the wall. In all examples, for the direct problem, the special interval $0.0^\circ \leq \phi \leq 180^\circ$ is divided into 1000 intervals, the spatial increments is chosen as $\Delta\phi = 0.18^\circ$, Eqs. (12) and (13) are applied to obtain the $\beta_i = \delta_i^3 \sin\phi_i$ at the nodes of the wall. Finally, the liquid film thickness distribution at some specific position where the sensors were assumed installed is obtained by the direct method, this values then being used as the simulated measured liquid film thickness δ, and let $\beta = \delta^3 \sin\phi$ to predict the unknown conditions of the wall in the inverse analysis.

In all examples, the simulated liquid film thickness ($\beta_i = \delta_i^3 \sin\phi_i$) is presumed to contain measurement errors. In other words, the random errors are added to the exact value of β, which is computed from the solution of direct problem. Thus, it can be written as

$$\bar{T}_{\text{simulated}} = \bar{T}_{\text{exact}} + \bar{T}_{\text{error}} = \bar{T}_{\text{exact}}(1 + \sigma) \tag{19}$$

where σ is the random error of the β. Letting ω to be the random error of the measurement, the relationship between σ and ω is $\sigma = \omega^3$. The measurement errors caused by the interpolation of the measuring instruments, uncertainty due to calibration, fluctuation in sensor reading during measurement, and the effect of condense film surface waves.

In the simulation, the accuracy of the estimation of unknown conditions from the knowledge of the $\beta_i = \delta_i^3 \sin\phi_i$ at measurement points are examined. As a result, the estimated solutions without containing measurement error ($\omega = 0$) converged to the solutions solved by the finite-difference method for all examples. Furthermore, the solutions are unique through the proposed verifying method. Detailed descriptions for the problem are presented as follows:

Example 1. The saturation temperature of the vapor is 100 °C. The liquid film properties are taken as $\mu = 0.282 \times 10^{-3}\,\mathrm{N\,s/m^2}$, $h_{fg} = 2258\,\mathrm{kJ/kg}$, $g = 9.81\,\mathrm{m/s^2}$ and $\rho = 840\,\mathrm{kg/m^3}$, which represent the water. The spatial variation of the strength of the wall heat flux $q(\phi)$ is taken as

$$q(\phi) = 10\,000\,(\mathrm{W/m^2}) \quad 0.0^\circ \leq \phi \leq 90^\circ$$

$$q(\phi) = 7500\,(\mathrm{W/m^2}) \quad 90.0^\circ \leq \phi < 180^\circ$$

For this example, the estimated heat flux $q(\phi)$ is expressed by two coefficients, $a_1 = 10\,000\,\mathrm{W/m^2}$ is the value of $q(\phi)$ at spatial grid which located along the ϕ axial from $\phi = 0.0^\circ$ to 90° and a_2=7500 $\mathrm{W/m^2}$ is the value of $q(\phi)$ at spatial grid which located along the ϕ axial from $\phi = 90.0^\circ$ to 180°. The value of $\zeta_i(\phi)$ is equal to 1. Fig. 2 shows the distribution of the condensate film thickness along the horizontal elliptical surface. The estimated values, without considering the measurement errors, are presented in Table 1, and give a very good approximation for two measurement points (the measured position is $\phi = 1.8^\circ$ and 18°).

Table 1 also shows a comparison of the estimated wall heat flux for measurement error $\omega = 10.00$, and 21.54% (the correspondence error σ equals 0.1 and 1.0%, respectively)

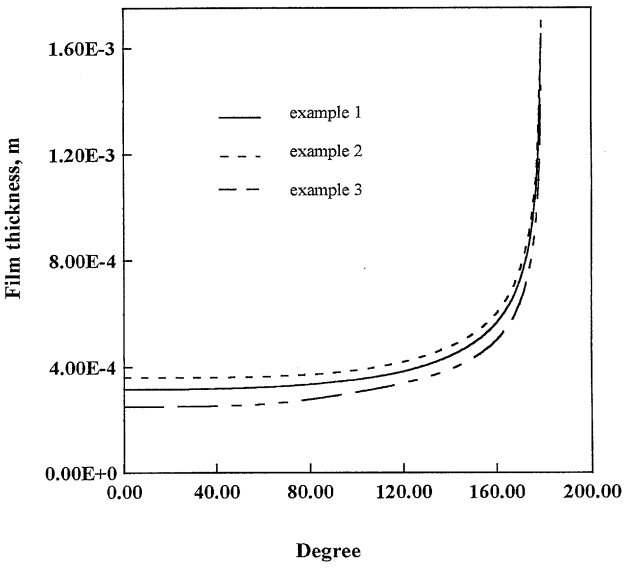

Fig. 2. Condensate film thickness along elliptical surface.

Table 1
Estimates of the wall heat flux for Example 1 with measurement errors (N, the number of measurement point)

Sensor location (°)	Range (°)	$q_{exact}(\phi)$	$q_{estimate}(\phi)$		
			$\omega = 0\%$	$\omega = 10.00\%$	$\omega = 21.54\%$
$\phi = 1.8, 18$ ($N = 2$)	0–90	10000	10000	–	–
	90–180	7500	7500	–	–
$\phi = 1.8, 18, 108, 126$ ($N = 2$)	0–90	10000	10000	10015	10145
	90–180	7500	7500	7375	6257

with four measurement points. The measured position located at $\phi = 1.8°$, 18°, 108° and 126°. The maximum discrepancies in heat flux at the wall are 1.67 and 16.57% for the $\omega = 10.00$ and 21.54% error cases, respectively.

In this example, the estimated values contain measurement errors, the magnitude of the discrepancies in the estimated surface heat flux is directly proportional to both the size of measurement error and the condensate film thickness.

Example 2. The variation of the wall heat flux $q(\phi)$ over space is presented as

$$q(\phi) = 5000 + 5000(1 + \cos\phi)\ (\mathrm{W/m^2}) \quad 0.0° \le \phi < 180°$$

the other conditions being the same as Example 1.

The estimated heat flux $q(\phi)$ is expressed by 21 coefficients. The value of $\zeta_i(\phi)$ is equal to 1. The distribution of the condensate film thickness along the horizontal elliptical surface is shown in Fig. 2 also.

The estimated values, excluding measurement error, are presented in Fig. 3. One observes a very good approximation for 22 measurement points ($N = 22$, the measured position being equally located along the ϕ-axial from 4.68° to 175.68°, one per every 9°, and located at $\phi = 0.18°$, 177.84°). For 21 measurement points case, large film thickness (the position being located at $\phi = 172°$ and 180°) make the estimated results deviate from the exact solution.

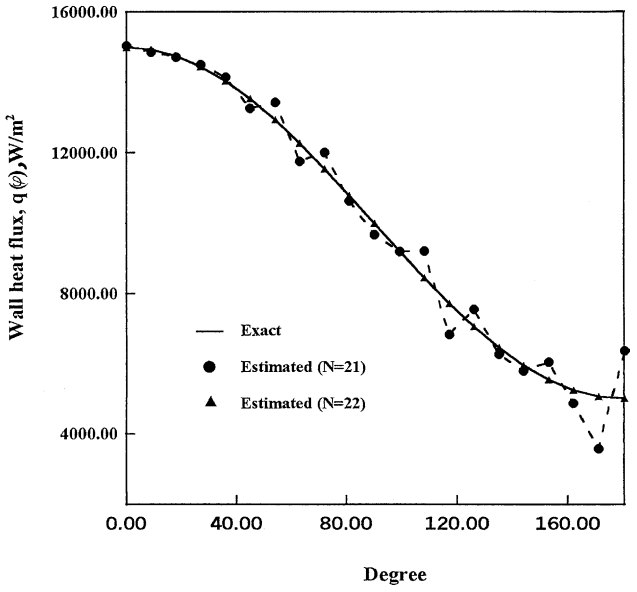

Fig. 3. Estimated wall heat flux for Example 2 without measurement error.

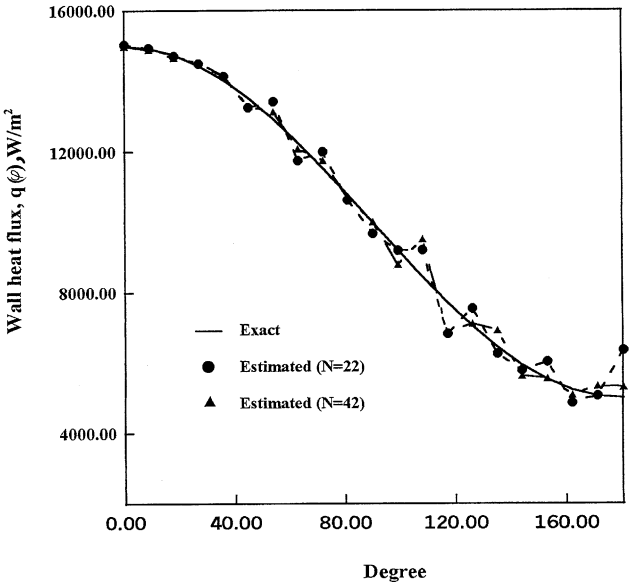

Fig. 4. Estimated wall heat flux for Example 2 with measurement error ($\omega = 10\%$).

Fig. 4 shows a comparison of the respective estimated wall heat flux for measurement points $N = 22$, and $N = 42$ ($N = 42$ with 22 measurement points being the same as in the excluding-measurement-error case, the other 20 sensors being located along the ϕ-axial from 11.34° to 173.34°, one per every 9°, and located at $\phi = 2.77°$) with measurement error $\omega = 10.00\%$ (correspondence errors σ equal to 0.1%). The estimated value is shown in the figure, is seen to oscillate. The oscillation becomes more severe for film thickness response data as increases. The maximum discrepancies in heat flux at the wall are 9.57 and 2.35% for the $N = 22$ and $N = 42$ cases, respectively. The magnitude of the discrepancies in the surface heat flux is directly proportional to the thickness of condensate film, and requires a greater number of measurement points to increase the accuracy of the estimates.

Fig. 5 shows a comparison of the respective estimated wall heat flux for measurement error $\omega = 10.00$, and 21.54% (correspondence errors σ equal to 0.1 and 1.0%,

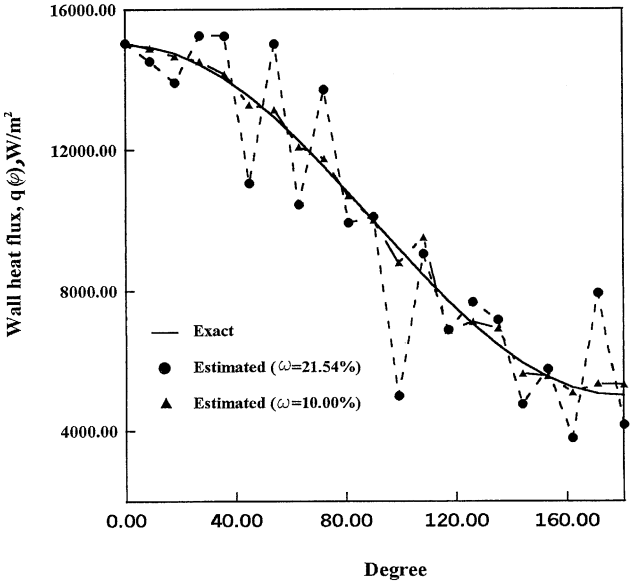

Fig. 5. Estimated wall heat flux for Example 2 with 42 measurement points.

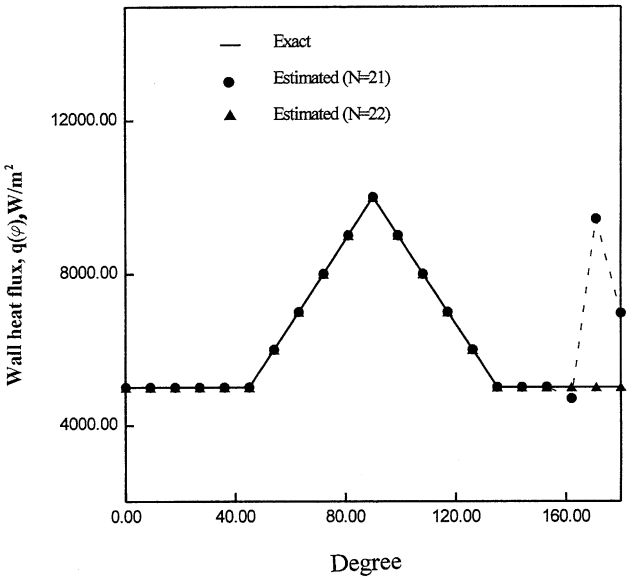

Fig. 6. Estimated wall heat flux for Example 3 without measurement error.

respectively) with 42 measurement points (the measured positions being same as above). The estimated value is shown in the figure. The oscillation becomes more severe for film thickness response data as measurement error increases. The maximum discrepancies in heat flux at the wall are 2.35 and 25.12% for the $\omega = 10.00$ and 21.54% error cases, respectively.

Example 3. The spatial variation of the wall heat flux $q(\phi)$ is taken as follows:

$$q(\phi) = 5000\,(\mathrm{W/m^2}), \quad 0.0^\circ \le \phi \le 45^\circ$$

$$q(\phi) = 5000\left[1 + \frac{\phi - 45^\circ}{45^\circ}\right](\mathrm{W/m^2}), \quad 45^\circ \le \phi \le 90^\circ$$

$$q(\phi) = 10000\left[1 - \frac{\phi - 45^\circ}{45^\circ}\right](\mathrm{W/m^2}), \quad 90^\circ \le \phi \le 135^\circ$$

$$q(\phi) = 5000\,(\mathrm{W/m^2}), \quad 135^\circ \le \phi \le 180^\circ$$

the other conditions are the same as Example 1.

The estimated heat flux $q(\phi)$ is expressed by 21 coefficients. The value of $\zeta_i(\phi)$ is equal to 1. The distribution of the condensate film thickness along the horizontal elliptical surface is shown in Fig. 2 also.

The estimated values, without measurement error, are presented in Fig. 6. One observes a very good approximation for 22 measurement points ($N = 22$, the measured position being the same as Example 2 for the excluding-measurement-error case). For 21 measurement points case, large film thickness (the position being located at $\phi = 172^\circ$ and 180°) make the estimated results deviate from the exact solution.

Fig. 7 shows a comparison of the respective estimated wall heat flux for measurement error $\omega = 10.0\%$ (correspondence errors σ equal to 0.1%) with 22 measurement points, and $\omega = 17.1\%$ (correspondence errors σ equal to 0.5%) with 42 measurement points (the measured positions being same as above). The estimated value is shown in the figure. The oscillation becomes more severe for film thickness response data as measurement error increases. The maximum discrepancies in heat flux at the wall are 16.4 and 20.09% for the $\omega = 10.0$ and 17.1% error cases, respectively.

In the above examples, the estimated values, excluding measurement errors, are obtained with the use of only a few

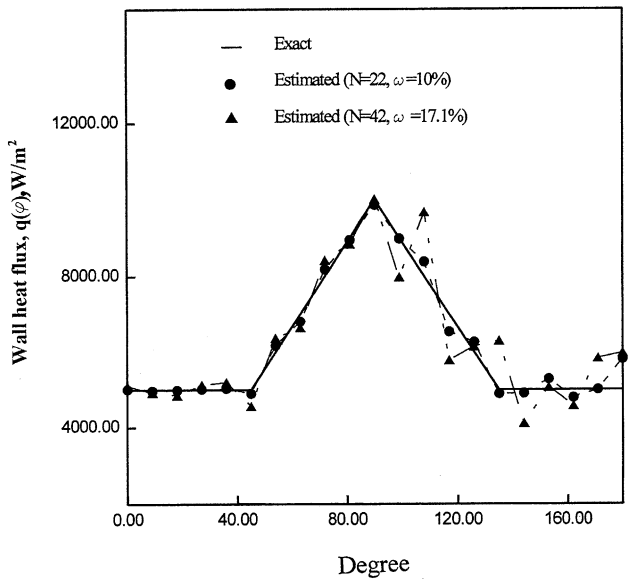

Fig. 7. Estimated wall heat flux for Example 3 with measurement error.

of measurement points. Nevertheless, a very good approximation of the wall heat flux is obtained. When considering the measurement errors, the magnitude of the discrepancies in the surface heat flux is directly proportional to the size of measurement error. Thus, greater measurement error requires a greater number of measurement points to increase the accuracy of the estimates.

The inverse matrix **R** (Eq. (18)) may become ill-conditioned for situations with high measurement error and when measured at locations with thick film, which means that the estimated values are very sensitive to any error in the liquid film thickness measurement, and may even become unstable. The sensitivity depends on the type of problem being solved (i.e. the governing equation and its boundary conditions), the position at which thickness of the condensed film is measured, and the measurement error. The present results confirm that the inverse values are extremely sensitive to measurement error, sensor location and number of sensors, that is ill-posed nature of IHCP, as mentioned by Beck et al. [6] and Hensel [17].

4. Conclusion

The proposed method is successfully applied to the solution of a simulated inverse filmwise condensation problem involving estimating surface heat flux. A direct inverse formulation is constructed using a reverse matrix, which is derived from the governing equation and boundary conditions. Three examples are used to evaluate the robustness of the proposed method. From the results, it appears that, discounting measurement error, the proposed method yields an accurate solution, even when using only a few points of measurement. When measurement errors are included, in order to enhance stability and accuracy, film thickness data require more measurement points at locations closer to the surface. This proposed inverse analytic method requires no prior information regarding the functional form of the unknown quantities, requires no initial guess, and the number of iterations in the calculation process is limited to 1. This implies that the present model offers a great deal of flexibility. Further, the results confirm that the proposed method is effective and efficient for inverse heat condensation problems. Although the difficulty of the measurement of the film thickness in practice is acknowledged, it is possible to use the proposed method to estimate the wall heat flux in film condensation on a surface.

References

[1] W. Nusselt, Die oberflachen-kondensation des wasserdampfes, Zeitschrift des Vereines Deutscher Ininuere 60 (1916) 541–569.
[2] C.Y. Wang, J.Z. Joseph, Yi. Feng, Laminar film condensation of pure saturated vapors on horizontal elliptical tubes, in: Proceedings of the International Symposium on Phase Change Heat Transfer, May 20–31, 1988, pp. 307–311.
[3] S.A. Yang, C.K. Chen, Filmwise condensation on nonisothermal horizontal elliptical tubes with surface tension, J. Thermophys. 7 (4) (1993) 729–731.
[4] S.A. Yang, Investigation of filmwise condensation heat transfer on horizontal plates, elliptical tubes and ellipsoids, Doctor Thesis, National Cheng-Kung University, Tainan, Taiwan, 1993.
[5] S.A. Yang, C.K. Chen, Laminar film condensation on a horizontal elliptical tube with variable wall temperature, ASME J. Heat Transfer 116 (1994) 1046–1049.
[6] J.V. Beck, B. Blackwell, C.R. St. Clair, Inverse Heat Conduction: III. Posed Problem, Wiley, New York, 1985.
[7] G.J. Stolz, Numerical solutions to an inverse problem of heat conduction for simple shapes, ASME J. Heat Transfer 82 (1960) 20–26.
[8] R.G. Arledge, A. Haji-Sheikh, An iterative approach to the solution of inverse heat conduction problems, Numer. Heat Transfer 1 (1978) 365–376.
[9] G. Krzysztof, M.J. Cialkowski, H. Kaminski, An inverse temperature field problem of the theory of thermal stresses, Nucl. Eng. Des. 64 (1981) 169–184.
[10] N. D'Souza, Numerical solution of one-dimensional inverse transient heat conduction by finite difference method, ASME Paper No. 75-WA/HT-81, 1975.
[11] G.W. Krutz, R.J. Schoenhals, P.S. Hore, Application of the finite-element method to the inverse heat conduction problem, Numer. Heat Transfer 1 (1978) 489–498.
[12] J.V. Beck, B. Litkouhi, C.R. St. Clair Jr., Efficient sequential solution of the nonlinear heat conduction problem, Numer. Heat Transfer 5 (1982) 275–286.
[13] C.H. Huang, J.Y. Wu, Two-dimensional inverse problem in estimating heat fluxes of an enclosure with unknown internal heat source, J. Appl. Phys. 76 (1) (1994) 133–141.
[14] A.A. Tseng, T.C. Chen, F.Z. Zhao, Direct sensitivity coefficient method for solving two-dimensional inverse heat conduction problems by finite-element scheme, Numer. Heat Transfer B 27 (1995) 291–307.
[15] C.Y. Yang, C.K. Chen, The boundary estimation in two-dimensional inverse heat conduction problems, J. Phys. D 29 (1996) 333–339.
[16] Y.T. Yang, P.T. Hsu, C.K. Chen, A 3D inverse conduction problem approach for estimating heat flux and surface temperature on a hollow cylinder, J. Phys. D 30 (1997) 1326–1333.
[17] E. Hensel, Inverse Theory and Applications for Engineers, Prentice-Hall, Englewood Cliffs, NJ, 1991.